Measurements of Kinematic Properties of the Cervical Spine Using Magnetic Resonance Imaging

Eriksson, Joakim; Bojsen-Møller, Finn; Juul-Kristensen, Birgit; Finsen, Lotte; Bolling, Max; Ståhlberg, Freddy; Larsson, Elna-Marie; Johansson, Gerd

1998

Document Version:
Early version, also known as pre-print

Submitted paper

Measurements of Kinematic Properties of the Cervical Spine Using Magnetic Resonance Imaging

Joakim Eriksson[1], Finn Bojsen-Møller[2], Birgit Juul-Kristensen[3], Lotte Finsen[3], Max Bolling[4], Freddy Ståhlberg[4,5], Elna-Marie Larsson[5], and Gerd Johansson[1].

[1]Div. of Ergonomics, Lund Institute of Technology, Lund, Sweden
[2]Dept. of Anatomy and Biomechanics, University of Copenhagen, Copenhagen, Denmark
[3]Danish National Institute of Occupational Health, Copenhagen, Denmark
[4]Dept. of Radiation Physics, University Hospital, Lund, Sweden
[5]Dept. of Radiology, University Hospital, Lund, Sweden

ABSTRACT

This paper presents kinematic data on the cervical and upper thoracic spine, based on measurements made on 20 Scandinavian healthy, female volunteers, aged 22-58 years (mean age 40.4). The aim was to provide anatomical *in vivo* data, primarily intended as data for biomechanical modelling of the upper spine. Together with the measurements of standard anthropometric body dimensions, magnetic resonance imaging (MRI) was used to capture the inner anatomy for each subject. A rigid linkage system is described for the vertebrae C_I-T_{VI}, with one link per vertebra. Measurements include link lengths, link rotations, and antero-posterior endpoints of the spinous process. Furthermore, correlation coefficients are calculated between link lengths and anthropometric measurements. Also presented are regression equations for each link length, with stature as a predictor. Using additional images of lower accuracy, a sub-study (N=15) investigated possible differences in link length and link rotation between non-flexion and maximum-flexion of the neck. The differences in link lengths were significant ($p<0.05$) for only 1 of the 16 measured links (C_{II}-T_X). Regarding link rotation, differences were significant for 4 links (C_V-T_I). Finally, the precision of the results was evaluated using two methods: by using a phantom for determining the geometrical uncertainties caused by the scanner; and by comparing results between two repeated measurement rounds. The phantom test revealed that the pixel resolution and magnetic field inhomogenities had only a minor influence on the results. The comparisons of repeated measurements revealed a significant difference for the links C_I and C_{II}, indicating that the landmarks for determining the occipital and C_I/C_{II} joints were the most difficult to identify on the images.

Relevance: The forwarded kinematic data for the upper spine may be used for biomechanical models, for instance, which could help explain the causes of musculoskeletal disorders.

Keywords: Cervical spine, MRI, Kinematics, Anthropometry, Biomechanics, Link length, Link rotation.

INTRODUCTION

Discomfort and disorders of the neck-shoulder region belong to one of the most common work-life problems, and it seems that problems in this body region are especially prominent among women (1, 2). The prevalence of neck-shoulder disorders appears to be more frequent among people with long exposure to repetitive and heavy work (3, 4). Neck-shoulder diseases are a common reason behind long periods of sick-leave and early retirement, constituting an increasing cost for the society. However, there is today very limited knowledge about the actual mechanisms behind the emergence of pain/disorders in this region. It is most likely that physical aspects such as work-load and repetitiveness are interacting with psycho-social and individual factors, which affect the emergence of pain/disorder to an unknown extent.

Nevertheless, it should be of vital importance to learn more about the physical load on the musculoskeletal system, and biomechanical modelling is one such technique (5), which can help to simulate how different body postures, movements, and if present, external forces, affect various tissues of the musculoskeletal system. Biomechanical models of the cervical spine, beside being used in an occupational context, e.g. by Finsen (6) and Harms-Ringdahl et al. (7), have also been extensively used in impact/trauma simulations, among others by Williams and Belytschko (8), and by Panjabi (9).

It is important to emphasise that biomechanical models are products of major simplifications of the musculoskeletal system. Furthermore, the validity and precision of biomechanical models are, of course, dependent on the quality of the data on which these models are based. In a review article on cervical spine biomechanics, Huelke and Nusholtz (10) conclude that further investigations employing dynamic, three-dimensional models are needed, and to accomplish this there is a need for further knowledge about a wide range of parameters, such as certain dynamic response data, as well as anatomical data.

The development of computer-based tomography techniques, such as computed x-ray tomography (CT) and magnetic resonance imaging (MRI), has made it possible to perform measurements on living subjects, thus providing the possibility to supplement/refine available biomechanical data without many of the problems associated with cadaver studies. Over the last 10-15 years, several studies have been performed with CT and MRI with the objective to measure musculoskeletal properties, such as moment arms, and cross-sectional areas of muscles. Regarding tomography investigations of the trunk, the lumbar region has to date attracted particular interest (11, 12, 13, 14, 15, 16, 17), whereas similar measurements of the neck region using these methods, are sparse.

A study on 20 Scandinavian healthy, female volunteers has been performed with the aim to provide *in vivo* measurements of the neck-shoulder region, thus providing data for future, more detailed biomechanical models. An MR scanner was used to capture the inner anatomy, together with the measurements of standard anthropometric dimensions.

This paper will present data of the linkage system of the neck, such as link lengths, link rotations, antero-posterior endpoints of the spinous process, and also the correlation between link lengths and anthropometric measurements. A sub-study will investigate possible differences in link length and link rotation between non-flexion and maximum-flexion of the neck. Furthermore, the way geometrical errors of the MR scanner affect the results, will also be assessed.

METHOD AND MATERIALS

Subjects

The study involved 20 Scandinavian female volunteers, aged 22-58 years. Their occupations were typically clerks, administrators and students, i.e. no industrial workers or occupations with a heavy or repetitive workload. A requirement for inclusion in the study was that the subjects did not currently, or in the recent past, have any pain or disorders of the neck or shoulders. In order to deselect such individuals, the Nordic standardized questionnaire on disorders was handed out to each subject on two occasions: first a few weeks prior to, and a second time just before the MR examination. A description of this questionnaire for self-assessment of discomfort/disorders can be found in Kourinka et al. (18). Furthermore, some standard criteria for allowing an MR examination without risks had to be followed: The subject was not to be pregnant, have any metal implants, or suffer from claustrophobia. The study was approved by the ethical committee of the Lund University Hospital.

Image Acquisition

Image acquisition was carried out on a Siemens Magnetom Vision 1.5 T whole body MR scanner. In order to optimize the signal-to-noise ratio (SNR) in the investigated areas, all measurements were performed using a cp-spine-array coil. The inner diameter of the MR scanner was 60 cm, and during acquisition, the subjects were instructed to lie as still as possible inside the scanner.

Based on three pilot measurement sessions, a protocol was developed consisting of three sequences for the upper spine, and four sequences for the shoulder region. The sequences varied concerning body posture, area of interest, slice orientation, as well as in image quantity/quality (e.g. number of images, field-of-view, matrix size, type of sequence, etc.). Prior to some of the sequences, the subjects were re-positioned into another posture. The sequences also had to be preceded by a "scout", i.e. rapid pre-sequence images to correctly set the orientation and position of the slices. In total, the scanner-time for each subject was approximately 1 hour, which was judged as a maximum, for the comfort of the subjects.

The image analysis in this paper will focus on the three sequences that captured the upper spine, hereafter referred to as sequence I, II and III:

- *Sequence I* was obtained in a normal supine posture, covering the cervical/thoracic spine in the sagittal plane from eye-level to about the seventh thoracic vertebra. A T2-weighted turbo spin echo sequence with an acquisition time of 3 minutes and 16 seconds was used. The field-of-view (FOV) was 280 mm and the matrix size was 300x512, giving a pixel size of 0.93x0.55 mm. The matrix information was interpolated to an image of 512x512 pixels. The number of slices was 11, each with a thickness of 3 mm and an interslice gap of 0.3 mm.

- *Sequence II* and *sequence III* were obtained with a normal, non-flexed neck posture, and with a flexion near maximum, respectively. This paper will analyze the scout sequence images in the sagittal plane, in order to determine possible differences in link length and link rotation between these two postures. These images had a matrix size of 128x256, and a FOV of 450 mm, resulting in a pixel size of 3.52x1.76 mm. The matrix information was interpolated to an image of 256x256 pixels. It should be observed that these images were of substantially poorer quality than

those from sequence I, since they were primarily intended for aligning/positioning the actual sequence[1].

Investigation of geometrical errors

One possible source of geometrical errors in the resulting MR images is distortion due to local magnetic field inhomogenities. Scanner inhomogenities result in an erratic signal distribution, primarily in the outer edges of the FOV, which may cause errors in measurements of distances and areas.

Figure 1 shows a phantom which was designed to investigate the geometric errors, especially regarding large FOVs. The phantom consisted of a plastic tube filled with a water solution (0.1 mM $MnCl_2$ and 9 g/l NaCl), and with plastic pins intersecting the tube at intervals of 50 or 100 mm. The distance between the two most peripheral pins was 500 mm. Acquisitions were made with the sequence that was employed in this work. Distances between the pin at the center of the phantom and the most peripheral pin in view were measured on the images and compared to the real value.

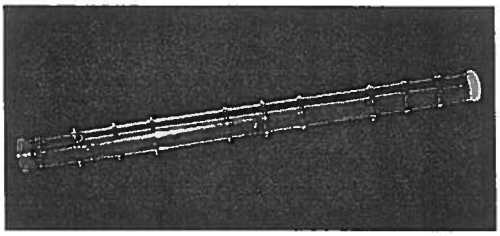

Figure 1. The phantom used for investigating geometric distortions, especially concerning peripheral areas in large Fields-of-View (up to 500 mm).

Image analysis

The image analysis was made using the programs PS2D (Promentus Software) and Photoshop (Adobe Inc.), which were hosted on standard PC and Macintosh computers.

The following mechanical model of the upper spine was assumed: Each vertebral bone was to be represented by a rigid link. Thus, a model of the head, neck and upper thorax (to the 10th vertebra) consisted of a chain of 18 interconnected links. For each link, the center-of-rotation was at the interconnection to its caudally adjacent link. These interconnection points were located at the centroid of each vertebral disk.

[1] The full-quality images of sequences II and III were obtained in a transverse orientation, with the aim to determine cross-sectional muscle areas and moment arms.

The images of sequence I were used to quantify link length, link rotation, and end-points of the spinous process. Figure 2a shows a typical mid-sagittal image from sequence I. The pixel coordinates were registered for some anatomical landmarks from the mid-sagittal images:

1. Posterior end of the margin of the foramen magnum
2. Anterior end of the margin of the foramen magnum
3. Posterior arch of the atlas
4. Anterior arch of the atlas
5. Vertex of the dens axis

For each vertebra, the following landmarks were quantified from the mid-sagittal images:

6. Vertebral body - anterior, superior tip
7. Vertebral body - posterior, superior tip
8. Vertebral body - posterior, inferior tip
9. Vertebral body - anterior, inferior tip
10. The most anterior tip of the spinous process
11. The most posterior tip of the spinous process

Figure 2b shows the anatomical landmarks listed above.

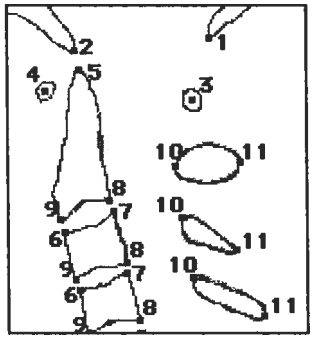

Figure 2a. (left) A typical mid-sagittal image from sequence I.

Figure 2b. (above) The anatomical landmarks which were used for the image analysis.

The location of the centroid point of a disk in the mid-sagittal plane (i.e. assumed to be the center-of-rotation) was calculated from the landmarks in the following way: first by calculating a mid-point between the anterior and posterior tips of the vertebral bodies. The centroids were then calculated as mid-points between the inferior anterior-posterior mid-point of vertebra *i*, and the superior anterior-posterior mid-point of vertebra *i+1*. As an exception, the center-of-rotation of the atlas was calculated as the intersection of two lines: the line between the anterior and posterior arches of the atlas, and the mid-line through dens axis. For the skull, its center-of-rotation was assumed to be located on a line from the anterior end to the posterior end of foramen magnum, at a distance that corresponds to the center-point of the occipital condyles. Unfortunately, the occipital condyles were difficult to locate in our image material. Instead, the distance at which the condyles could be expected was approximated as 21% of the total distance on the line from anterior to the posterior end of foramen magnum. This approximation was based on actual measurements of 10 skulls from the collection at the Department of Anatomy, University of Copenhagen.

Given the coordinates for the centers of rotation, the link length is the linear distance between two centers, and the link rotation is the slant relative to its caudally adjacent link. It should be observed that link rotation here refers to rotation in the sagittal plane, which would be equivalent to flexion/extension using anatomical terminology.

Because of the poorer quality of the scout images of sequence II and III (see Figure 3) compared to those of sequence I, it was found that interpolating the center-point of a disk from adjacent vertebral bodies did not improve the accuracy of the localization. Instead, the disk centers were located directly on the images.

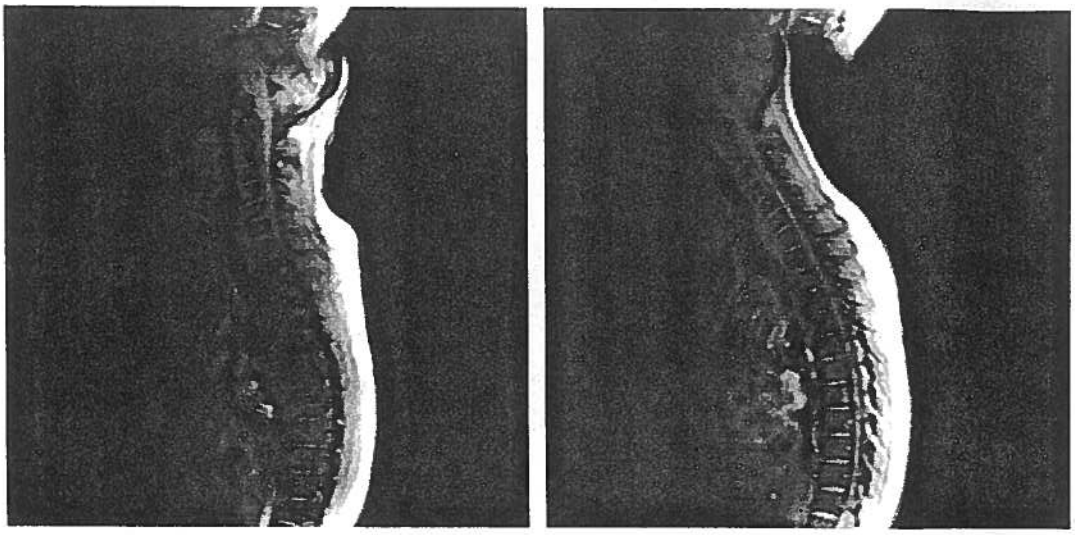

Figure 3. To the left: a typical scout image of sequence II (neck in non-flexed posture), and to the right: a typical scout image of sequence III (neck in forced flexed posture).

Anthropometrics

Anthropometric measurements were performed using an anthropometer for height and width measurements, a measuring tape for circumferences, and a digital scale for the weight measurements. For the height, width and circumference dimensions presented in this paper, one can estimate a measuring error of maximum 5 mm.

Statistics

Normal distributions were assumed for the anthropometric dimensions, as well as the anatomical measures of link length, link rotation and antero-posterior endpoints of the spinous process. The results are presented with their mean, standard deviation, and standard error of the mean. Furthermore, correlation coefficients were calculated between the link lengths, and also between link lengths and the anthropometric dimensions.

Linear regressions were calculated for estimated link lengths using an anthropometric dimension as a predictor. The numerical values presented are the intercept, slope, adjusted coefficient of determination (Adj. R^2), and standard error of estimate. Also the p-values of the f-distributions calculated by ANOVA are presented.

Paired t-tests were used to investigate differences in link lengths and link rotations between a flexed and a non-flexed neck position. The level of significance was set to $p<0.05$.

Assessment of precision

The precision in the results was assumed to be mainly affected by two factors: (a) the geometrical uncertainties of the scanner, and (b) the manual location of landmarks on the images.

Regarding (a), the geometrical uncertainties of the scanner, the phantom described above was used to estimate the geometrical error c. Given c, one can approximate how much this uncertainty contributes to the variance in the measurements.

An observed pixel coordinate x is assumed to follow a rectangular distribution (the y-direction is similar), which has the variance:

$$V(x) = \frac{c^2}{12}$$

In the analysis of sequence I, the centers-of-rotation are interpolated from 4 coordinates, and thus the variance becomes a quarter of the above:

$$V(x_{CR}) = \frac{c^2}{48}$$

By using the Gauss-approximation, the variance V and the deviation D of the link length L (i.e. the distance between two centers-of-rotation) can be approximated as:

$$V(L) \approx 2 * \frac{c^2}{48} = \frac{c^2}{24} \quad \Rightarrow \quad D(L) = \sqrt{V(L)} = 0.204c$$

Similarly, the link rotation R is determined by the position of three adjacent centers-of-rotation CR_1, CR_2 and CR_3. Assuming that angles are typically small (less than 0.3 radians, and thereby arctan(x)≈x), the variation can be simplified as:

$$V(R) \approx V\left(\left(\frac{x_{CR3} - x_{CR2}}{y_{CR3} - y_{CR2}}\right) - \left(\frac{x_{CR2} - x_{CR1}}{y_{CR2} - y_{CR1}}\right)\right)$$

Using the Gauss – approximation :

$$V(R) \approx \left[\left(\frac{1}{y_{CR2} - y_{CR1}}\right)^2 + \left(\frac{1}{y_{CR2} - y_{CR1}} + \frac{1}{y_{CR3} - y_{CR2}}\right)^2 + \left(\frac{1}{y_{CR3} - y_{CR2}}\right)^2\right] \cdot \frac{c^2}{48}$$

The y-distances for the links C_{II} to T_{VI} typically range between 15 to 30 mm. Thus, calculating with a "worst case" of 15 mm, the variance V and the deviation D would be:

$$V(R) \approx \frac{6}{225} \cdot \frac{c^2}{48} = \frac{c^2}{1800} \quad \Rightarrow D(R) \approx \frac{c}{42.4} \; [radians]$$

Regarding (b), the manual localization of the joint-centers on the images, the precision of this was investigated by comparing results (link lengths and link rotations) between two repeated measurements. Paired t-tests were then performed to identify significant differences between the two measurement rounds.

RESULTS

Anthropometrics

The subjects - numbered from 1 to 20 - are presented in Table 1 with their age, weight, stature, and a selection of some standard anthropometric dimensions. The mean, standard deviation and standard error of the mean have been calculated for these data.

Table 1. Age, weight and a selection of standard anthropometric measurements of the subjects, enumerated 1 to 20 (weight is in kilograms and body dimensions are in millimeters).

Subject no.	#1	#2	#3	#4	#5	#6	#7	#8	#9	#10	#11	#12	#13	#14	#15	#16	#17	#18	#19	#20	Mean	SD	N	SE_M
Age	49	29	27	58	39	46	44	35	28	30	31	33	26	56	22	53	55	54	48	44	40.4	11.7	20	
Weight	51.9	61.2	65.7	67.6	52.7	56.7	86.7	50.7	81.8	64.3	67	60.4	69	55.4	62.4	63	72	65	79.5	70.4	65.2	9.7	20	2.2
Stature	1630	1710	1680	1580	1700	1555	1735	1615	1670	1725	1620	1750	1695	1560	1640	1665	1620	1650	1640	1675	1656	55.3	20	12.4
Trochanter height	840	905	825	780	830	820	845	785	850	890	795	930	870	870	835	865	810	875	840	895	848	40.2	20	9.0
Femur lateral epicondule height	470	510	425	445	450	455	490	420	450	490	435	495	475	470	480	470	455	470	450	460	463	23.4	20	5.2
Acromion to midfinger-tip	725	745	760	685	670	680	740	675	725	715	710	755	720	675	710	730	710	710	705	735	714	26.7	20	6.0
Vertex to C7	245	250	260	245	235	240	255	245	220	265	235	230	240	215	240	220	225	210	210	215	235	16.5	20	3.7
C7 to L4/L5	390	420	450	400	460	370	455	450	450	440	430	410	380	425	390	435	415	440	450	475	427	29.1	20	6.5
Biacromial breadth	370	360	365	370	345	340	390	340	360	375	380	380	360	355	415	380	390	360	370	390	370	18.7	20	4.2
Upper arm length	335	340	345	300	325	310	350	320	350	340	330	350	340	315	315	345	345	340	325	340	333	14.7	20	3.3
Elbow to midfinger-tip	440	430	455	420	410	410	460	405	430	445	440	450	465	425	440	450	415	425	435	455	435	17.7	20	4.0
Hand length	200	180	180	175	170	170	200	160	175	185	180	185	190	185	195	180	180	165	160	180	180	11.4	20	2.6
Palm length	115	110	110	105	105	100	125	95	100	120	100	110	115	110	105	100	105	100	100	105	107	7.7	20	1.7
Sitting height	-	855	-	-	900	-	-	900	-	-	860	880	855	820	860	875	825	860	865	885	865	24.3	13	6.7
Neck circumference	330	330	345	325	303	360	410	305	370	325	320	320	335	335	320	345	350	370	340	350	339	25.0	20	5.6
Tragion to vertex	150	120	120	125	135	130	140	125	130	140	130	140	130	130	175	130	130	140	130	140	135	12.1	20	2.7
Acromion to C7	205	205	210	205	196	185	210	205	210	210	220	220	200	205	220	220	230	210	225	220	211	10.7	20	2.4

Measurements on the images

In Table 2, the mean, standard deviation and standard error of mean of the link lengths have been calculated for each vertebral body, C_I to T_{VI}. The link lengths and link rotations were calculated as an average of the two measurement rounds. The rotation of each link is presented as an angle relative to the orientation of its caudally adjacent link. Thus, the series of positive values in the upper part and negative values in the lower part correspond to the cervical lordosis and the thoracic kyphosis, respectively.

Table 2. The link lengths and rotations, representing the vertebrae C_I to T_{VI}. The rotation of a link is presented as an angle relative to the orientation of its caudally adjacent link, and the direction is clockwise in the sagittal plane, seen from the left side.

	Link length				Link rotation			
	Mean [mm]	SD [mm]	N	SE_M [mm]	Mean [°]	SD [°]	N	SE_M [°]
C_I	11.6	1.1	20	0.3	30.8	7.7	20	1.7
C_{II}	33.0	2.4	20	0.5	9.6	3.7	20	0.8
C_{III}	16.4	1.2	20	0.3	0.6	3.2	20	0.7
C_{IV}	16.1	1.1	20	0.2	-0.3	3.9	20	0.9
C_V	15.7	1.0	20	0.2	1.8	4.0	20	0.9
C_{VI}	15.9	1.4	20	0.3	7.1	4.0	20	0.9
C_{VII}	17.6	1.1	20	0.2	4.7	1.9	20	0.4
T_I	19.0	1.0	20	0.2	1.2	3.6	20	0.8
T_{II}	19.9	1.1	20	0.2	-5.3	3.1	20	0.7
T_{III}	20.0	1.0	20	0.2	-3.4	2.7	20	0.6
T_{IV}	20.5	1.1	20	0.3	-4.2	2.6	19	0.6
T_V	20.9	1.0	19	0.2	-6.0	2.4	12	0.7
T_{VI}	20.8	1.2	12	0.3	-8.4*	5.6	3	3.2

*The rotation of T_{VI} is relative to the orientation of T_{VII}.

Regarding the precision of the repeated measurements, the differences between the first and second measurements were largest for the links C_I and C_{II}. This can be explained by the fact that the landmarks for determining the occipital and C_I/C_{II} joints were the most difficult to identify on the images. The differences in mean link length were 1.0 mm for C_I, and -0.8 mm for C_{II}. A t-test (paired) showed that these differences were significant ($p<0.05$). For the remaining links, the mean link length differed only between -0.1 and 0.1 mm (T_{VI} slightly more: -0.3 mm), and these differences were not significant. Regarding link rotation, the mean values of links C_I and C_V differed -4.7° and -1.2°, respectively (both significant, $p<0.05$). The remaining links had no significant differences in rotation, ranging between -1° and 1°.

Table 3 shows the correlation coefficients between link lengths. In general, the strongest correlations can be found for the closest adjacent links, for example between C_{IV} and C_V.

In Table 4, correlation coefficients have been calculated between link lengths and the anthropometric measurements. All correlations were generally positive except for age, and the strongest correlations can be found for sitting height and stature, indicating that these two measurements would be the most appropriate for linear regression equations to predict the link lengths. Measurements on the upper limb showed better correlations than lower limb measurements. Height measurements generally correlated better than weight, circumference and width measurements.

Figure 4 shows linear regressions for the lengths of link C_I to T_{VI}. Stature, rather than sitting height, was selected as the predicting parameter, because sitting height was measured only on 13 subjects, and also because stature data are more frequent in the literature. Each diagram in Figure 4 presents the plots of the measurement, regression coefficients, adjusted R^2 value and the standard error of estimate. Also presented are the p-values of the f-distributions calculated by ANOVA. All regressions, except for C_I and T_{III}, were significant ($p<0.05$).

Table 3. Correlation coefficients between link lengths.

	C_I	C_{II}	C_{III}	C_{IV}	C_V	C_{VI}	C_{VII}	T_I	T_{II}	T_{III}	T_{IV}	T_V	T_{VI}
C_I	-	0.24	0.41	0.36	0.47	0.30	0.41	0.49	0.32	0.38	0.27	-0.01	0.07
C_{II}	0.24	-	0.65	0.60	0.58	0.75	0.56	0.58	0.62	0.48	0.69	0.76	0.50
C_{III}	0.41	0.65	-	0.85	0.75	0.66	0.66	0.59	0.55	0.47	0.56	0.56	0.47
C_{IV}	0.36	0.60	0.85	-	0.87	0.75	0.77	0.71	0.57	0.38	0.41	0.39	0.36
C_V	0.47	0.58	0.75	0.87	-	0.81	0.85	0.74	0.59	0.37	0.42	0.42	0.24
C_{VI}	0.30	0.75	0.66	0.75	0.81	-	0.77	0.66	0.63	0.36	0.48	0.56	0.33
C_{VII}	0.41	0.56	0.66	0.77	0.85	0.77	-	0.82	0.79	0.46	0.60	0.48	0.63
T_I	0.49	0.58	0.59	0.71	0.74	0.66	0.82	-	0.83	0.71	0.74	0.50	0.52
T_{II}	0.32	0.62	0.55	0.57	0.59	0.63	0.79	0.83	-	0.66	0.73	0.50	0.72
T_{III}	0.38	0.48	0.47	0.38	0.37	0.36	0.46	0.71	0.66	-	0.74	0.63	0.56
T_{IV}	0.27	0.69	0.56	0.41	0.42	0.48	0.60	0.74	0.73	0.74	-	0.70	0.73
T_V	-0.01	0.76	0.56	0.39	0.42	0.56	0.48	0.50	0.50	0.63	0.70	-	0.73
T_{VI}	0.07	0.50	0.47	0.36	0.24	0.33	0.63	0.52	0.72	0.56	0.73	0.73	-

Table 4. Correlation coefficients between link lengths and the anthropometric measurements.

	C_I	C_{II}	C_{III}	C_{IV}	C_V	C_{VI}	C_{VII}	T_I	T_{II}	T_{III}	T_{IV}	T_V	T_{VI}
Stature	0.34	0.74	0.71	0.70	0.54	0.62	0.54	0.53	0.56	0.30	0.55	0.47	0.67
Weight	-0.06	0.40	0.09	0.36	0.33	0.41	0.25	0.19	0.22	0.01	0.16	-0.12	-0.17
Age	0.07	-0.33	-0.41	-0.32	-0.31	-0.54	-0.29	-0.05	-0.12	-0.08	-0.13	-0.53	-0.59
Trochanter height	0.26	0.19	0.13	0.12	0.01	0.14	0.16	0.09	0.16	-0.21	0.19	-0.07	0.37
Femur lateral epicondule height	0.33	0.15	0.06	0.05	0.03	0.02	0.04	0.06	0.09	-0.13	0.13	-0.25	0.26
Acromion to midfinger-tip	0.38	0.60	0.27	0.36	0.33	0.63	0.40	0.48	0.38	0.17	0.47	0.28	0.41
Vertex to C7	0.08	0.42	0.36	0.30	0.36	0.47	0.13	0.25	0.13	0.24	0.11	0.34	0.00
C7 to L4/L5	-0.05	0.44	0.44	0.52	0.33	0.40	0.51	0.46	0.53	0.42	0.49	0.43	0.32
Biacromial breadth	0.25	0.18	0.07	0.13	0.15	0.32	0.22	0.33	0.38	0.29	0.33	0.09	0.04
Upper arm length	0.30	0.72	0.36	0.41	0.34	0.52	0.51	0.50	0.53	0.28	0.60	0.42	0.62
Elbow to midfinger-tip	0.49	0.43	0.30	0.35	0.34	0.57	0.24	0.32	0.33	0.17	0.25	0.04	0.18
Hand length	0.49	0.28	0.20	0.14	0.21	0.34	0.13	0.17	0.19	0.15	0.17	-0.10	-0.06
Palm length	0.33	0.52	0.37	0.33	0.26	0.39	0.06	0.19	0.19	0.11	0.18	-0.07	-0.13
Sitting height	0.34	0.44	0.84	0.79	0.79	0.66	0.78	0.60	0.67	0.44	0.50	0.55	0.80
Neck circumference	0.03	0.32	-0.05	0.15	0.24	0.23	0.24	0.29	0.24	0.07	0.36	-0.34	-0.11
Tragion to vertex	0.31	-0.09	0.25	0.07	0.15	0.09	0.23	0.21	0.31	0.27	0.28	0.01	0.29
Acromion to C7	0.11	0.22	-0.04	0.02	-0.02	0.19	0.17	0.23	0.33	0.28	0.30	0.30	0.08

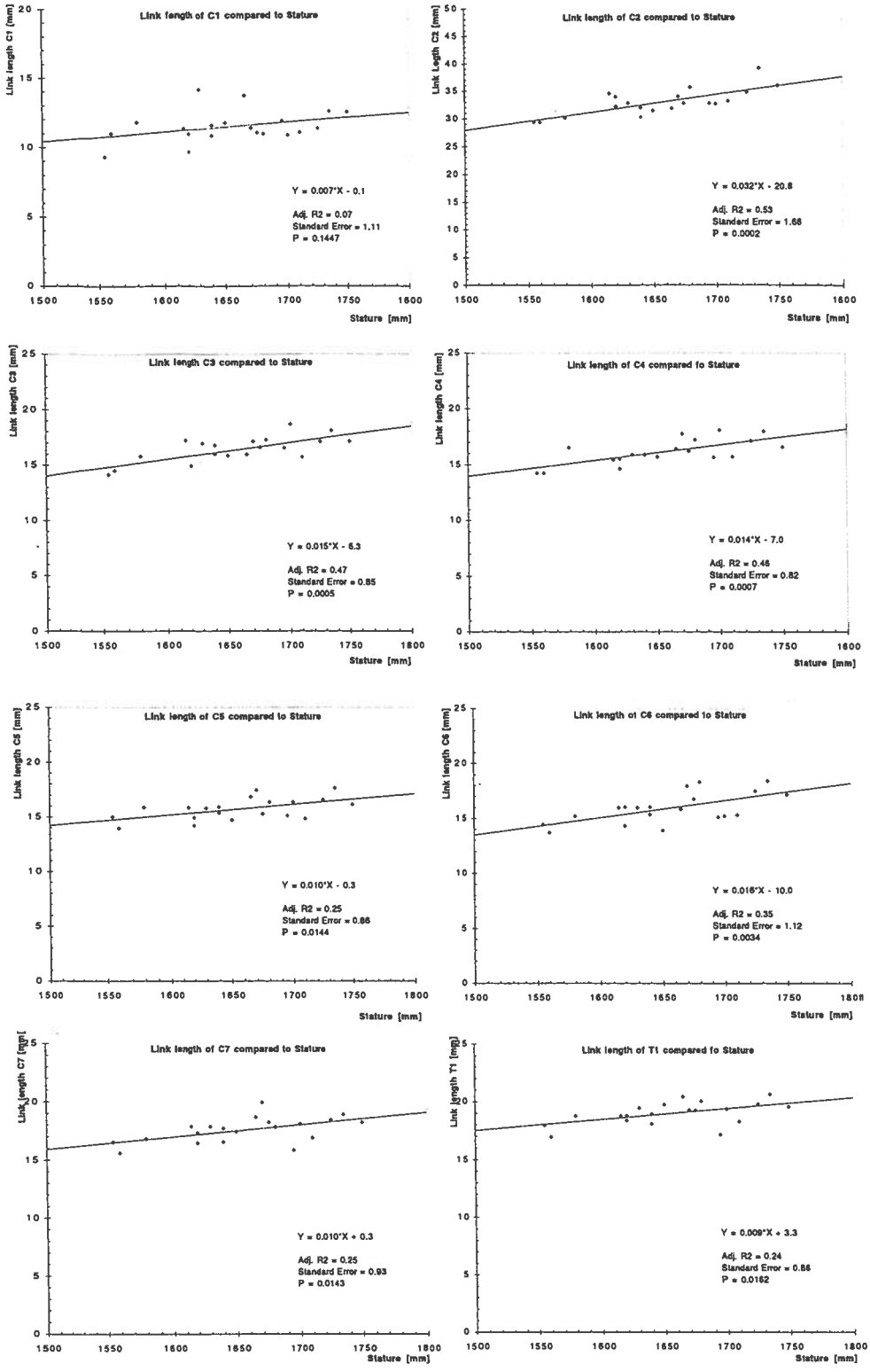

Figure 4. Data plots and regression equations of link lengths with stature as independent variable

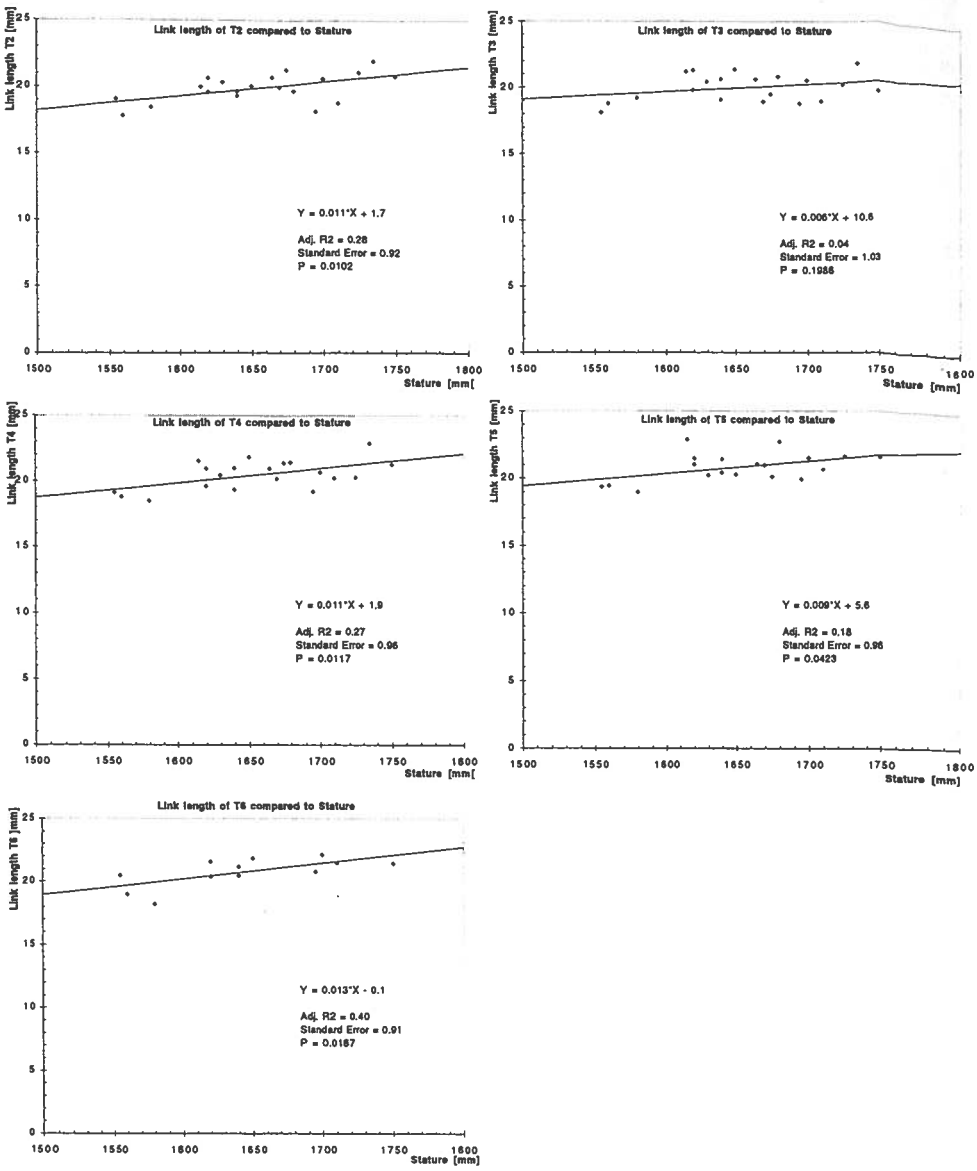

Figure 4. Data plots and regression equations of link lengths with stature as independent variable

Table 5 presents the coordinates for the anterior most tip and the posterior most tip of the spinous process of C_{II} to T_{VI}, as viewed from the mid-sagittal images (i.e. landmarks #10 and #11 as illustrated in Figure 2b). The xy-coordinates are expressed in each link's local frame-space, where origo is at the center-of-rotation, the x-axis is perpendicular to the link (posterior direction), and the y-axis is parallel to the link (cranial direction). Also presented for each vertebra is the distance *d* from the posterior endpoint of the spinous process to the corresponding center of rotation.

Table 5. Anterior and posterior endpoints of the spinous process, expressed as coordinates for each link's local frame-space. The positive x-axis is in a posterior direction, and the positive y-axis is in a cranial direction. For each link, *d* is the distance from the posterior endpoint of the spinous process to the center of rotation.

	Anterior end					Posterior end						
	x [mm]		y [mm]			x [mm]		y [mm]		*d* [mm]		
	Mean	SD	Mean	SD	N	Mean	SD	Mean	SD	Mean	SD	N
C_{II}	23.9	1.5	10.4	3.5	20	38.3*	2.2	9.7	3.9	39.7	1.6	20
C_{III}	22.8	1.4	9.6	2.6	20	34.0	1.9	1.6	3.8	34.2	1.8	20
C_{IV}	22.3	1.2	10.9	2.2	20	34.4	2.5	1.9	3.6	34.6	2.5	20
C_{V}	22.2	1.2	11.1	2.4	20	38.6	2.9	1.5	4.2	38.8	2.9	20
C_{VI}	22.0	0.9	13.0	1.5	20	44.3	2.5	2.8	3.8	44.5	2.6	20
C_{VII}	22.2	1.0	13.7	1.9	20	49.2	2.7	0.4	3.7	49.3	2.8	20
T_{I}	23.7	1.2	11.6	1.5	20	50.2	2.5	-5.2	2.9	50.6	2.4	20
T_{II}	24.4	1.4	10.8	1.5	20	48.6	2.5	-10.0	4.8	49.8	2.3	20
T_{III}	25.7	1.2	11.4	1.7	20	49.3	2.2	-9.0	5.1	50.4	2.3	20
T_{IV}	27.0	1.5	11.9	1.6	20	48.1	2.6	-12.6	5.3	50.0	2.4	19
T_{V}	28.0	1.8	12.8	2.1	19	47.0	2.4	-16.2	5.0	50.0	1.6	16
T_{VI}	29.0	1.6	13.3	1.3	6	45.0	3.6	-21.2	6.6	50.2	3.0	6

*The mid-sagittal image slice (of 3 mm) may possibly have got into the interspace of the bifid process of C_{II}, which would result in a measurement smaller than the actual distance.

Table 6 shows the differences in link length between a normal supine posture and a posture in which the neck was supported to produce near maximum flexion. As seen in Table 6 the differences in link lengths are typically less than one millimeter, which is actually below the pixel resolution for these images. A t-test (paired) showed that significant ($p<0.05$) differences in link length between a flexed and a non-flexed position was found only for T_{II}. Regarding the differences in link rotation, one can note that the differences are most prominent around the lowest cervical links: C_{V} through T_{I} had differences with significant levels ($p<0.05$). The fluctuating differences for the thoracic links are most probably caused by the limited visibility and resolution of the image material.

Table 6. Link length and link rotation comparisons between a normal (non-flexed) and a flexed neck posture. Rotational direction is clockwise in the sagittal plane seen from left. N=15.

	Length [mm]					Rotation [°]				
	Normal		Flexed		Difference	Normal		Flexed		Difference
	Mean	SD	Mean	SD		Mean	SD	Mean	SD	
C_{II}	28.1	3.7	26.6	3.9	-1.5	3.4	5.5	1.0	6.1	-2.4
C_{III}	16.9	0.9	16.0	1.8	-0.9	0.5	7.3	0.0	6.4	-0.4
C_{IV}	15.9	1.4	17.1	1.8	1.2	1.5	6.7	-0.6	7.7	-2.1
C_{V}	15.7	1.3	16.2	2.0	0.6	2.0	5.1	-4.7	5.8	-6.6*
C_{VI}	16.5	1.4	17.1	1.4	0.6	9.2	7.4	2.1	11.5	-7.1*
C_{VII}	17.8	0.9	17.9	2.1	0.2	3.9	5.9	-2.4	8.3	-6.3*
T_{I}	19.4	1.5	19.6	1.5	0.1	1.3	5.0	-3.5	6.7	-4.8*
T_{II}	20.1	1.3	19.1	1.0	-1.0*	-7.6	4.9	-4.9	7.1	2.7
T_{III}	19.6	1.6	19.5	2.2	-0.1	-1.4	5.7	-5.6	5.2	-4.2
T_{IV}	20.5	1.5	20.7	2.1	0.2	-8.3	5.6	-6.3	9.4	1.9
T_{V}	20.5	1.1	21.0	1.5	0.5	-4.3	4.5	-8.3	6.3	-4.1
T_{VI}	22.3	1.8	21.7	2.8	-0.6	-5.2	4.6	-4.2	7.5	1.0
T_{VII}	21.1	1.6	22.0	1.7	0.9	-5.5	3.6	-6.7	6.2	-1.2
T_{VIII}	22.0	1.6	22.9	1.7	0.9	-4.3	4.4	-2.6	5.7	1.7
T_{IX}	22.3	1.5	22.9	1.5	0.6	-1.5	4.1	-2.6	6.1	-1.1
T_{X}	22.8	1.8	24.0	2.3	1.2					

*Difference significant at level $p<0.05$

Geometric uncertainties

Acquisitions using the phantom revealed that a FOV below 200 mm yielded an uncertainty below pixel-size, i.e. not detectable with this technique. With a FOV of 250 mm, the maximum geometrical error became approximately 1 mm. A FOV of up to 300 mm resulted in a maximum geometrical error of about 1.5 mm.

Applied to the images of sequence I: within a 200x200 mm central area (which typically includes C_{II} through T_{IV}) the geometrical error could be set to be the pixel-size of the images, i.e. c= 0.6 mm. In the surrounding area of up to 250x250 mm (which typically includes the occipital joint, the atlas, the dens axis, and T_V to T_{VI}), c can be up to 1 mm. For the remaining thoracic bones, an error c of up to 1.5 mm can be expected.

The measured link lengths had typical standard deviations of at least 1.0 mm. Using c=0.6 mm, the deviation caused by the measurement technique is approximately 0.1 mm. If deducting this deviation to get the "real" deviation caused by the normal biological variation, the adjusted *sd* becomes:

$$sd = \sqrt{1.0^2 - (0.204c)^2} = 0.99\ mm \quad \text{(using c = 0.6 mm)}$$

Apparently, the difference between the "real" deviation and the measured one is typically less than 1% (for T_y and T_{yI} it is about 2%), and therefore it is fairly safe to claim that the effect of scanner uncertainties can disregarded.

For the link rotations, the deviation becomes 0.014 radians (=0.8°) using a *c* value of 0.6 mm. If this deviation is deducted from the measured standard deviations, the compensated deviations differ by 2-4%. Consequently, also here it is fairly safe to disregard scanner uncertainties.

The scout images of sequence II and III carry substantially less precision: the FOV was here 450 mm (giving a pixel size of 1.76 mm), and the error ranges approximately from 2 mm at the centers of the images, towards 5 mm at their peripherals. Also, since the centers of the disk were here quantified directly from the images, the deviation of link lengths *D(L)* and rotations *D(R)* would then be (using c=2 mm):

$$V(L) \approx 2 * \frac{c^2}{12} \quad \Rightarrow \quad D(L) = \sqrt{V(L)} \approx 0.408c = 0.82\ [mm]$$

$$V(R) \approx \frac{6}{225}\frac{c^2}{12} \quad \Rightarrow \quad D(R) = \sqrt{V(R)} \approx 0.05c = 0.09\ [radians]$$

DISCUSSION

The measurements in this work are primarily intended for rigid linkage models, especially where a linkage-refinement level of one link per vertebral body is of interest. The presented kinematic data of the upper spine was based on images in the sagittal plane, and concerns link lengths, link rotations, and antero-posterior endpoints of the spinous process. The spinous process endpoints are given as coordinates relative the local frame-space of each link, and can be used, for instance, to estimate offsets between surface markers and the center of rotation. Also presented for each vertabra is the distance between the posterior tip of the spinous process and the center of rotation, which can be used to estimate moment arms in 2-dimensional (sagittal) biomechanic calculations.

The data presented may in future be supplemented with measurements on cross-sectional areas, volumes, and moment arms for different muscles, obtained from transverse images of the neck, which were also acquired in this study.

The precision of the results was evaluated by two methods: (a) by using a phantom to determine the geometrical uncertainties caused by the scanner; and (b) by comparing results between two repeated measurements. Method (a) revealed that the geometrical errors had a minor influence on the results: the difference between the "real" deviation due to biological variation, and the measured one was typically less than a few percent. Hence, it is fairly safe to disregard scanner uncertainties. Regarding (b), differences between the measurements were significant for the links C_I and C_{II}. This can be explained by the fact that the landmarks used to determine the occipital and C_I/C_{II} joints were the most difficult to identify on the images. For the remaining links, the mean link length differed typically between -0.1 and 0.1 mm, which was not significant.

The sub-study to investigate possible differences between non-flexion and maximum-flexion of the neck, used images with a lower resolution and containing more image artefacts. One can conclude that the differences in link lengths were mainly less than 1 mm, and hardly detectable using these images. The results would imply, though, that translations of the centers-of-rotation of the upper

spine are fairly small, and can in many cases be disregarded. For link rotation, the differences were largest for the links C_V through T_1. It should be noted, however, that the rotation in the occipital joint contributes substantially to the total flexion, but this was unfortunately not realiably measurable using the images to hand, due to scanner artefacts.

The correlation between different link lengths may be of interest for the prediction of a link length based on other link lengths. The correlations were generally between 0.4 to 0.8, and the correlation tended to increase the closer two links were to each other. The correlation of C_1, however, was substantially weaker than the others.

Regarding the results on correlation between link lengths and the anthropometric values, it may not be a surprise that height measurements - especially sitting height and stature - correlated better than weight, circumference, and breadth, and also that the correlations tended to be negative with age. However, the measurements vertex to C7, and C7 to L4/L5, were unexpectedly weaker correlated, as compared to sitting height. This is probably due to the uncertainties connected with measuring these anthropmetric dimensions.

It should be noted that all measurements on the MR images were taken for supine postures, which may result in compression of soft tissues, and a stretched-out S-curve. One should therefore be careful when comparing measurements made on a supine posture with those on an erect posture (19). Although it is assumed that such differences would be fairly small for this limited part of the upper spine, the results should be used with this in mind, especially regarding the link rotations.

Since the stature measurement (mean=166 cm; SD=5.5 cm) was employed as a predictor for link length estimates, it is of interest to compare the stature measurement with those in the literature: In Ingelmark & Lewin (20) mean stature is 164 cm (SD=6.6 cm), measured on Swedish women aged 25-49 years (N=112). Lewin (21) reports a mean of 164 cm (SD=6.2 cm) measured on Swedish female industrial workers (N=77). Jürgens et al. (22) present an international compilation projected to the year 2000, representing adults in the age group 25-45 years. For North-European females, the mean is 169 cm (SD=6 cm), where it should be noted that Jürgens et al. have calculated with a certain increase-factor in body growth due to the secular trend. Given these values, the subjects included in this study represent fairly well a North-European female population, regarding stature.

Several earlier studies provide extensive data of the size and form of the spine based on skeletons (23, 24). However, these measurements can not be directly compared with the results in this paper since they refer to the vertebral bones and not to the functional body links, i.e. distances between presumed centers of rotation.

Two of the most influential data sources for biomechanical modelling are the work of Dempster (25), and NASA's Anthropometric Source Book (26). Although the data sets in these publications are widely accepted and used, there are certain parts of the body which are described in less detail and uniformity. This applies, for instance, to various parts of the trunk. Furthermore, it should be observed that much of this data material is based on cadaver studies, for which a limited selection of specimens has been available (Dempster's original dismemberment study, for example, included 8 cadavers, of which all were males, and the known age ranged from 52 to 83 years). A well known concern about cadaver studies is the presumed differences compared to living tissue, for example the increase in circumferences due to the use of embalming fluids in order to compensate for dehydration, as well as other post-mortem effects (19). Hence, there are several advantages in performing anatomical measurements on the living.

The advantages of using MR for biomechanical investigations have been acknowledged in several earlier articles, such as Tracy et al. (14) and Wood et al. (17): It can be an excellent supplement to traditional cadaver studies in that it offers a unique accuracy and contrast for soft tissues such as muscles, tendons and ligaments, viewed on living subjects. At present, however, MR scanning is

relatively expensive and its accessibility for biomechanic/anthropometric studies may in many places be limited.

Compared with X-ray methods such as CT and plain radiography, MR has the advantage of not emitting any ionizing radiation, thus avoiding radiation exposure to healthy volunteers. On the other hand, radiographic images can be acquired more rapidly, which is advantageous, for instance, when investigating the variation of joint-positions during flexion/extension of the spine (27, 28, 29). In recent years, special MR-coils (e.g. for knees and elbows) for motion measurements have become available, but not with frame-rates as high as those achievable with radiography. Furthermore, the common horizontal-field MR units are restricted to supine postures/movements inside a cylinder, about 60 cm in diameter, whereas using plain radiography, one would be free to choose almost any posture/movement.

This study is confined to Scandinavian females, and in future work it would be of interest to gather similar information for the male population. It would also be interesting to compare the present results on a healthy population with a similar study on individuals with neck/shoulder disorders caused by exposure to a long working-life. In further biomechanic/anthropometric studies one could also investigate the potentials of comprehensive improvements of MR technology, such as rapid 3D-acquisition, and sequential acquisitions for certain body movements.

ACKNOWLEDGMENTS

The project was funded by the Swedish Council for Work Life Research.

REFERENCES

1 Westerling D, Jonsson BG. Pain from the Neck-Shoulder Region and Sick Leave. *Scand. J. Soc. Med.* 1980; 8: 131-136.

2 Ohlsson K. Neck and Upper Limb Disorders in Female Workers Performing Repetitive Industrial Tasks. PhD-thesis, Dept. of Occupational and Environmental Medicine, Lund University, Sweden, 1995.

3 Hagberg M, Wegman DH. Prevalence rates and odds ratios of shoulder-neck diseases in different occupational groups. *Br. J. of Industrial Medicine* 1987; 44: 602-610.

4 Ohlsson K, Attewell R, Skerfving S. Self-reported symptoms in the neck and upper limbs of female assembly workers. *Scand. J. of Work Environment and Health* 1989; 15: 75-80.

5 Hidalgo JA, Genaidy AM, Huston R, Arantes J. Occupational Biomechanics of the Neck: A Review and Recommendations. *J. of Human Ergol.* 1992; 21: 165-181.

6 Finsen L. Biomechanical Analyses of Occupational Work Loads in the Neck and Shoulders. PhD-thesis, National Inst. of Occupational Health, Denmark, 1995.

7 Harms-Ringdahl K, Ekholm J, Schüldt K, Németh G, Arborelius UP. Load Moments and Myoelectric Activity when the Cervical Spine is Held in Full Flexion and Extension. *Ergonomics* 1986; 29(12): 1539-1552.

8 Williams JL, BelytschkoTB. A Three-Dimensional Model of the Human Cervical Spine for Impact Simulation. *J. of Biomech. Engineering* 1983; 105: 321-331.

9 Panjabi MM. Three-Dimensional Mathematical Model of the Human Spine Structure. *J. of Biomechanics* 1973; 6: 671-680.

10 Huelke F, Nusholtz GS. Cervical Spine Biomechanics: A Review of the Literature. *J. of Orthopaedic Research* 1986; 4(2): 232-245.

11 Németh G, Ohlsén H. Moment Arm Lengths of Trunk Muscles to the Lumbosacral Joint Obtained *In Vivo* with Computed Tomography. *Spine* 1986; 11(2): 158-160.

12 Reid JG, Costigan PA, Comrie W. Prediction of Trunk Muscle Areas and Moment Arms by Use of Anthropometric Measures. *Spine* 1987; 12(3): 273-275.

13 McGill SM, Patt N, Norman RW. Measurement of the Trunk Musculature of Active Males Using CT Scan Radiography: Implications for Force and Moment Generating Capacity About the L4/L5 Joint. *J. Biomechanics* 1988; 21(4): 329-341.

14 Tracy MF, Gibson MJ, Szypryt EP, Rutherford A, Corlett EN. The Geometry of the Muscles of the Lumbar Spine Determined by Magnetic Resonance Imaging. *Spine* 1989; 14(2): 186-193.

15 Chaffin DB, Redfern MS, Erig M, Goldstein SA. Lumbar Muscle Size and Locations from CT Scans of 96 Women of Age 40 to 63 Years. *Clin. Biomechanics* 1990; 5(1): 9-16.

16 Hultman G, Nordin M, Saraste H, Ohlsén H. Body Composition, Endurance, Strength, Cross-sectional Area, and Density of MM Erector Spinae in Men With and Without Low Back Pain. *J. of Spinal Disorders* 1993; 6(2): 114-123.

17 Wood S, Pearsall DJ, Ross R, Reid JG. Trunk Muscle Parameters Determined From MRI for Lean to Obese Males. *Clin. Biomechanics* 1996; 11(3): 139-144.

18 Kourinka I, Jonsson A, Kilbom A, Vinterberg H, Biering-Sørensen F, Andersson G, Jørgensen K. Standardised Nordic Questionnaires for the Analysis of Musculoskeletal Symptoms. *Applied Ergonomics* 1987; 18(3): 233-237.

19 Clauser CE, McConville JT, Young JW. Weight, volume and center of mass of segments of the human body. Ohio: Aerospace Medical Research Laboratories, 1969.

20 Ingelmark BE., Lewin T. Anthropometrical studies on Swedish women in standing and sitting posture. *Acta Morphologica Neerlando-Scandinavica* 1968; 7(2): 167-178.

21 Lewin T. Anthropometric studies on Swedish industrial workers when standing and sitting. *Ergonomics* 1969; 12(6): 883-902.

22 Jürgens HW, Aune IA, Pieper U. International data on anthropometry. Geneva: International Labour Office, 1990.

23 Lanier RR. The Presacral Vertebrae of American White and Negro Males. *Am. J. Phys. Anthropology* 1939; 25(3): 341-420.

24 Francis CC. Dimensions of the Cervical Vertebrae. *Anatomical Record* 1955; 122: 603-609.

25 Dempster WT. Space requirement of the seated operator: Geometrical, kinematic and mechanical aspects of the body with special reference to the limbs. Ohio: Air Research and Development Command, Wright-Patterson Air Force Base, 1955.

26 NASA. Anthropometric source book Vol. 1, NASA Reference Publication 1024. Yellow Springs, Ohio: Webb Associates, 1978.

27 Pearcy M, Portek I, Shepherd J. Three-Dimensional X-ray Analysis of Normal Movement in the Lumbar Spine. *Spine* 1984; 9(3): 294-297.

28 Ogston NG, King GJ, Gertzbein SD, Tile M, Kapasouri A, Rubenstein JD. Centrode Patterns in the Lumbar Spine: Baseline Studies in Normal Subjects. *Spine* 1986; 11(6): 591-595.

29 Roozmon P, Gracovetsky SA, Gouw GJ, Newman N. Examining motion in the cervical spine I: imaging systems and measurement techniques. *J. Biomed. Eng.* 1993; 15: 5-12.